Dynamic reconfiguration of distribution network considering the uncertainty of distributed generation and loads

Qi Liu, Lihong Zhang, Xingquan Ji* and Huizhe Shi

College of Electrical Engineering and Automation, Shandong University of Science and Technology, Qingdao, China

This study presents a new methodology to perform the distribution network dynamic reconfiguration (DNDR), taking into consideration the stochastic variations of loads and distributed generation (DG) of power. To solve the heavy computational burden that exists in traditional algorithms of the DNDR, this study first establishes the nodal sensitivity models to calculate the nodal variations caused by nodal power variations. Then, the DNDR is executed utilizing a co-evolutionary algorithm with the goal of loss minimization. The stochastic power flow calculations (PFCs) based on the nodal sensitivity are performed in the DNDR to handle the power fluctuations of the DGs and loads. Finally, the modified IEEE 33-bus test system and a practical distribution system are used for simulations. The simulation results validate the quickness and effectiveness of the proposed DNDR method.

1 Introduction

1.1 Literature review

The distribution network reconfiguration (DNR) can adjust the network topology and improve the performance of distribution networks by combining the open/closed states of line switches. The goals of the DNR include reducing the power losses (Lotfi et al., 2020), improving system reliability (Kianmehr et al., 2019), enhancing system resilience (Sun et al., 2023), reducing voltage drops (Song et al., 2020), and managing energy (Gao et al., 2022a). The DNR plays an important role in the distribution automation of the system.

It is usually formulated as a complex non-linear optimization problem. The solution algorithms for the DNR include intelligent optimization algorithms, heuristic algorithms, and mathematical programming algorithms. Intelligent optimization algorithms, such as the genetic algorithm, honeybee mating optimization algorithm, particle swarm optimization algorithm, and harmony search algorithm, have been successfully applied in DNR (Roosta et al., 2019; Jakus et al., 2020; Lotfi and Ghazi, 2021; Hizarci et al., 2022). However, the tremendous amount of computation of intelligent optimization algorithms greatly limits their engineering applications. The heuristic algorithms can solve the DNR problem with high speed. In the study by Harsh and Das (2023), a two-stage heuristic algorithm based on the power flow analysis is used for DNR. Zhan et al. (2020) proposed the switch opening and exchange method for DNR. Recently, efficient mathematical programming algorithms, such as convex programming, have been

successfully applied in DNR. López et al. (2015) presented a mixed-integer second-order conic programming model for the DNR considering the reliability constraints. Sekhavatmanesh and Cherkaoui (2020) proposed a multi-step reconfiguration model of active distribution network restoration based on mixed-integer second-order cone programming.

Distributed generation (DG) technology has been developed rapidly in recent years due to its flexible and environment-friendly nature (Zheng et al., 2021a). However, when many DGs are connected to the system, the power fluctuation of DGs increases the risks of the distribution network operation (Zhang et al., 2023). Therefore, it is essential to take nodal power fluctuations into account in the DNR. Santos et al. (2022) considered the uncertainties of DGs and loads and carried out the DNR with the goal of reducing carbon emission costs. Raj and Kumar (2020) proposed a new DNR method based on affine arithmetic to handle the uncertainties of nodal powers. Haghighat and Zeng (2016) introduced continuous uncertainty sets and developed and solved a mixed-integer robust optimization model under a master–slave framework. Zheng et al. (2021b) presented an adaptive robust distribution network model for three-phase DNR.

1.2 Problem addressed

The distribution network dynamic reconfiguration (DNDR), which takes the time-varying load and constraint of the switch operation into account, is applicable for engineering applications. Considering the influence of forecast errors, the actual loads and DG in power deviate from the predicted data. When the uncertainty of nodal power is considered in the dynamic reconfiguration, the calculation burden is huge, which greatly limits its feasibility for engineering applications. In the study by Razavi et al. (2022), the stochastic DNDR based on the probability distance method is employed to shrink the scenario sets, and a self-adaptive modified crow search algorithm is introduced to find an optimal scenario. Gao et al. (2022b) established a stochastic dynamic reconfiguration model based on selected scenarios to address the uncertainties of the DGs and loads.

However, the number of switch operations is usually treated only as a constraint in existing dynamic reconfiguration approaches, which ignores the influence of the switch operation on the operational cost of distribution systems. When both the switch operational cost and nodal power fluctuation are considered in the DNDR, the computational burden is heavy, and it becomes difficult to obtain an effective solution quickly.

1.3 Contributions

To solve the problem of heavy computational burden that exists in the DNDR, a new methodology to perform the dynamic reconfiguration is proposed. The main contributions are as follows:

(i) The co-evolution algorithm is proposed to solve the dynamic reconfiguration model with the goal of loss minimization. The switch operational cost is considered in the DNDR, which can improve the operational costs of the distribution network effectively. The hash table is designed to store individuals' fitness, which can avoid extensive fitness calculations.

(ii) The effect of power fluctuation on the operation constraints is considered in the dynamic reconfiguration model to ensure operation security. The sensitivity models of nodal power to bus voltage are used to calculate the voltage and branch power, which can improve the computation efficiency of the DNDR.

1.4 Article organization

The rest of this article is organized as follows: Section 2 introduces the stochastic model of the DGs and loads. Section 3 introduces stochastic PFCs. Section 4 introduces the DNDR algorithm. Section 5 presents the simulation results, and the conclusions are drawn in Section 6.

2 Stochastic model of DGs and loads

It is supposed that the day-ahead active power of the wind turbine (WT) and photovoltaic (PV) power generation is predicted on the basis of weather conditions, and random variations of the active power output of wind power generation and PV power generation follows the normal distribution. The probability density function of the active power output of wind power generation P_{WT} and PV power generation P_{PV} can be described as:

$$f(P_{WT})\frac{1}{\sqrt{2\pi}\sigma_{P_{WT}}}exp\left(-\frac{\left(P_{WT}-\mu_{P_{WT}}\right)^2}{2\sigma_{P_{WT}}^2}\right),$$

$$f(P_{PV})\frac{1}{\sqrt{2\pi}\sigma_{P_{PV}}}exp\left(-\frac{\left(P_{PV}-\mu_{P_{PV}}\right)^2}{2\sigma_{P_{PV}}^2}\right)$$

where $\mu_{P_{WT}}$ and $\mu_{P_{PV}}$ are the mathematical expectations that are the predictive values of the active power output of wind and PV power generation, respectively; $\sigma_{P_{WT}}$ and $\sigma_{P_{PV}}$ are the standard deviations of P_{WT} and P_{PV}, respectively.

The reactive power of DG is supposed to follow the active power at the rated power factor.

The random variation of the active load follows a normal distribution, and the probability density function of the active load P_{LD} can be described as:

$$f(P_{LD})\frac{1}{\sqrt{2\pi}\sigma_{P_{LD}}}exp\left(-\frac{\left(P_{LD}-\mu_{P_{LD}}\right)^2}{2\sigma_{P_{LD}}^2}\right),$$

where $\mu_{P_{LD}}$ is the mathematical expectation that is the predictive value of the active load, and $\sigma_{P_{LD}}$ is the standard deviation.

It is supposed that the reactive load follows the active load by the rated power factor.

3 Stochastic power flow calculation

3.1 Sensitivity factors of bus voltage

The output power of the DGs is regarded as the negative load power in PFCs. The nodal equivalent power is the difference between the load power and DG output power:

FIGURE 1
Diagram of the simple distribution network.

FIGURE 3
Schematic of a simple distribution network.

FIGURE 2
Schematic of reconfiguration intervals.

FIGURE 4
Comparison and detection among the offspring chromosomes.
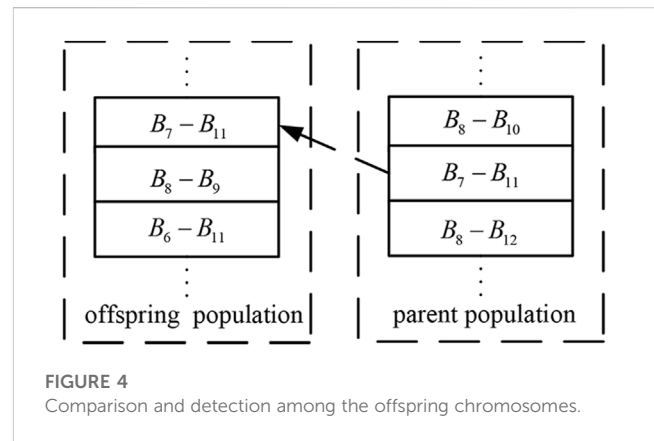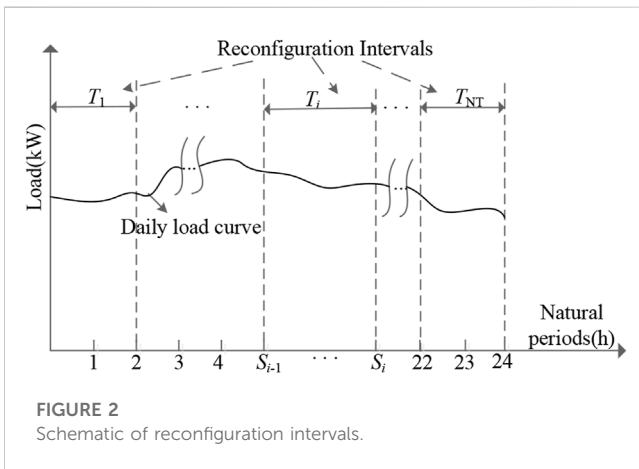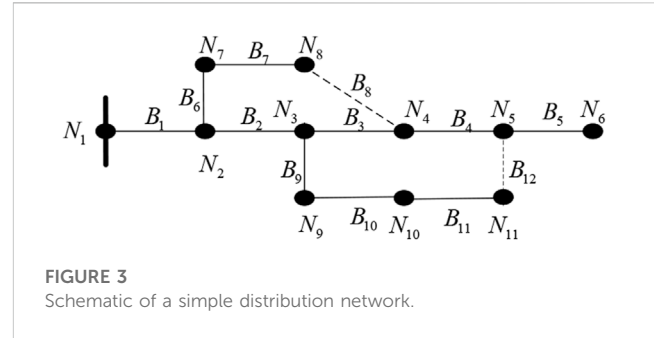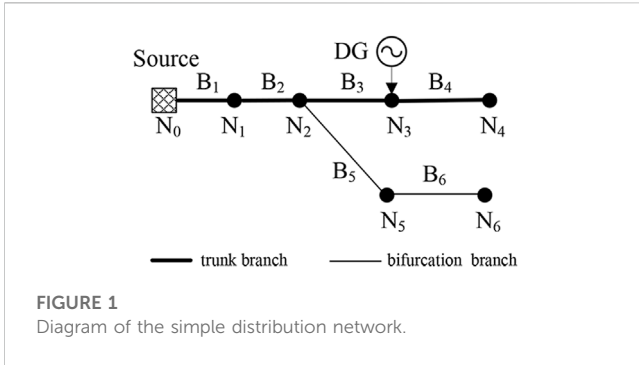
$$\begin{cases} P_{E.N_d} = P_{L.N_d} - P_{G,d} \\ Q_{E.N_d} = Q_{L.N_d} - Q_{G,d} \end{cases},$$

where $P_{G,d}$ and $Q_{G,d}$ are the active and reactive output power of the DG, respectively; $P_{L.N_d}$ and $Q_{L.N_d}$ are the active and reactive load power of node N_d, respectively; $P_{E.N_d}$ and $Q_{E.N_d}$ are the equivalent active and reactive power of node N_d, respectively.

In the process of calculating branch power, the power loss of the branch is temporarily ignored. Considering that the nodal voltages are close to their rated values at normal conditions, the per-unit value of the bus voltage is supposed to be 1. For the node $N_{i'}$, P_{C,N_i} and Q_{C,N_i} are defined as the nodal outfeed active power and reactive power. If a node on a trunk path is connected to one or more bifurcation branches, the sum of the nodal equivalent power on all bifurcation branches is defined as the nodal outfeed power, such as the node N_2 in Figure 1:

$$\begin{cases} P_{C,N_2} = P_{E.N_2} + P_{E.N_5} + P_{E.N_6} \\ Q_{C,N_2} = Q_{E.N_2} + Q_{E.N_5} + Q_{E.N_6} \end{cases},$$

where P_{C,N_2} and Q_{C,N_2} are the active and reactive nodal outfeed power of node N_2, respectively; $P_{E.N_2}$, $P_{E.N_5}$, and $P_{E.N_6}$ are the equivalent active power of nodes N_2, N_5, and N_6, respectively; $Q_{E.N_2}$, $Q_{E.N_5}$, and $Q_{E.N_6}$ are the equivalent reactive power of nodes N_2, N_5, and N_6, respectively.

For the node without bifurcation, the nodal outfeed power is equal to the nodal equivalent power, such as node N_1 in Figure 1:

$$\begin{cases} P_{C,N_1} = P_{E.N_1} \\ Q_{C,N_1} = Q_{E.N_1} \end{cases}.$$

For the general radial distribution network, when the outfeed power of node i changes, the voltage change ΔU_m of node m can be described as (Wang et al., 2018):

$$\Delta U_m = K^P_{i,m,vol} \cdot \Delta P_i + K^Q_{i,m,vol} \cdot \Delta Q_i,$$

where $K^P_{i,m,vol}$ and $K^Q_{i,m,vol}$ are the sensitivity factors of the voltage at node i to the nodal active and reactive power at node m, respectively. $K^P_{i,m,vol}$ and $K^Q_{i,m,vol}$ can be expressed as:

$$K^P_{i,m,vol} = \begin{cases} \sum_{B \in bpath_m} \dfrac{R_B}{U_B} & m \in npath_i \\ \sum_{B \in bpath_i} \dfrac{R_B}{U_B} & i \in npath_m, \\ K^P_{i,T_m,vol} & m \notin npath_i \cap i \notin npath_m \end{cases}$$

$$K^Q_{i,m,vol} = \begin{cases} \sum_{B \in bpath_m} \dfrac{X_B}{U_B} & m \in npath_i \\ \sum_{B \in bpath_i} \dfrac{X_B}{U_B} & i \in npath_m, \\ K^Q_{i,T_m,vol} & m \notin npath_i \cap i \notin npath_m \end{cases}$$

where U_B is the end node voltage of branch B; $bpath_i$ is the branch set from node i to the source node of the distribution network; $npath_i$ is the node set that contains all nodes from i to the source node on the path of power flow; T_m is the first node with laterals in
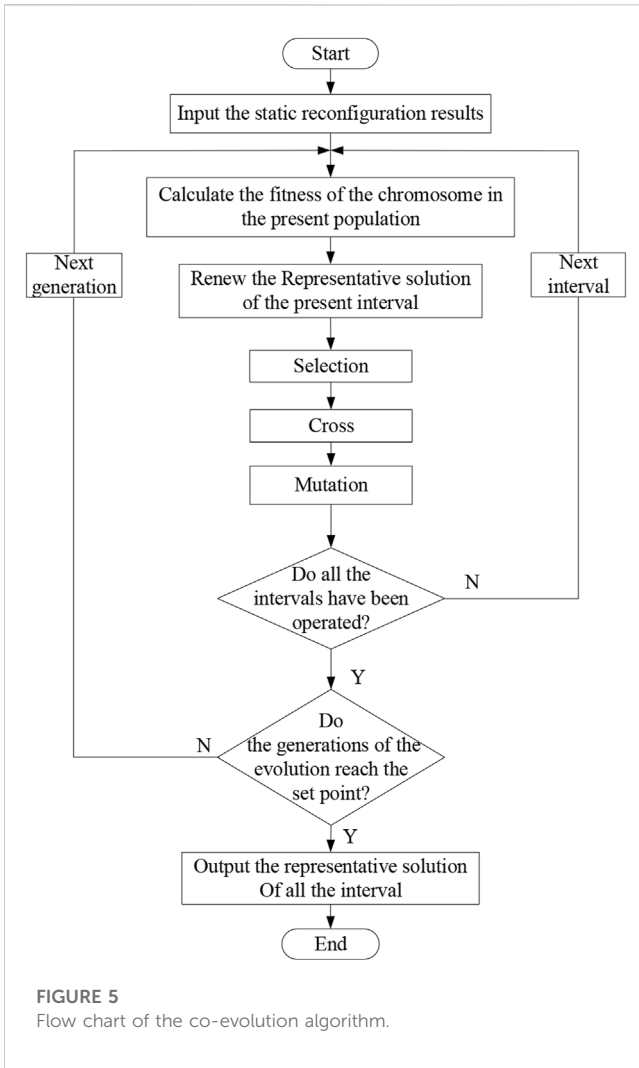
FIGURE 5
Flow chart of the co-evolution algorithm.

the node set from node m to the source node; R_B and X_B are the resistance and reactance of branch B, respectively.

3.2 Stochastic power flow calculation based on sensitivity model

The power of the load and DG is supposed to be constant within a period. First, according to the predicted load power and DG power, the node voltages and branch power are obtained through PFCs. The distribution network operation scenarios considering the power fluctuations of the DGs and loads are obtained by Latin hypercube sampling (LHS). In the generative distribution network operation scenarios, the difference between the predicted value and generative value of each node is used to calculate the change of the node voltages by the sensitivity model. Then, the nodal voltages are obtained by summing up the change of node voltages caused by stochastic variations of nodal power. Finally, the branch power and line losses are obtained by nodal voltages.

4 Dynamic reconfiguration of distribution network based on co-evolution algorithm

4.1 Time intervals division

Time intervals division can reduce the computation cost of dynamic reconfiguration. As shown in Figure 2, the daily load curve is divided into natural periods. Several successive natural periods form a reconfiguration interval in which the network topology remains unchanged.

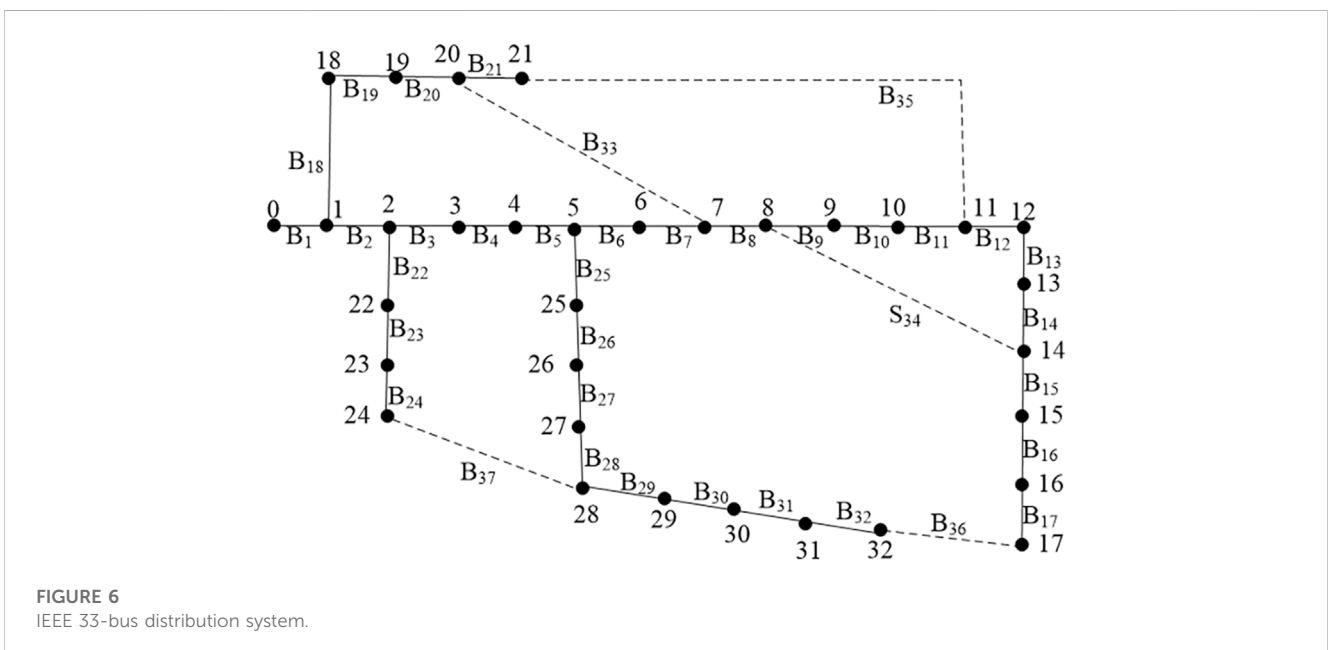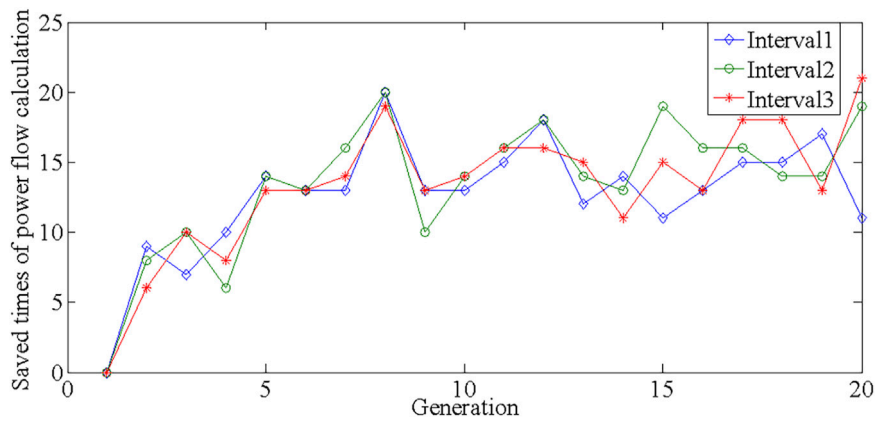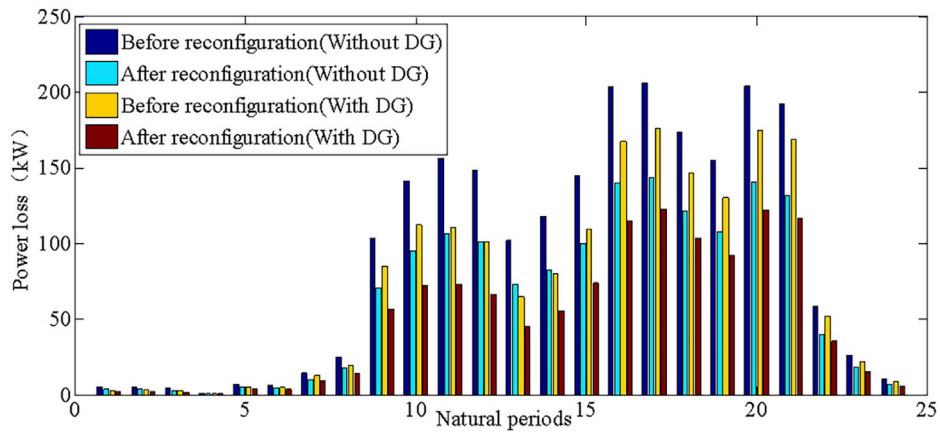The objective function of reconfiguration interval divisions can be described as:
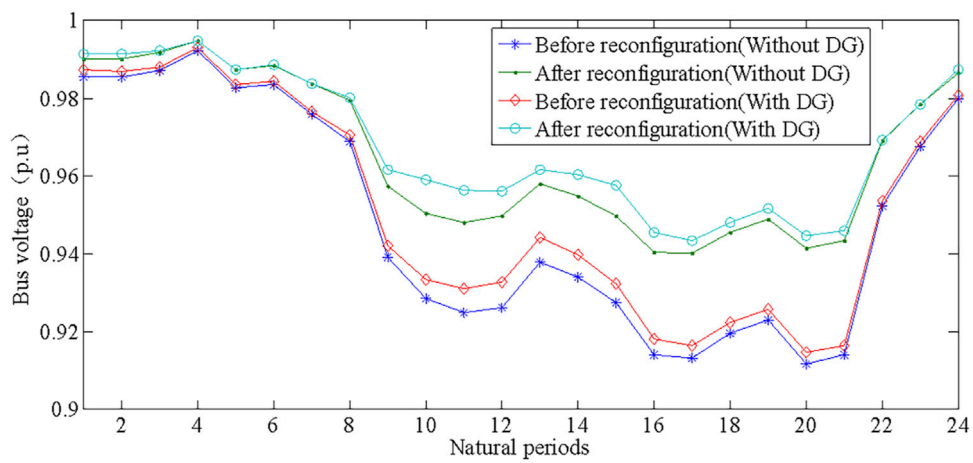

FIGURE 6
IEEE 33-bus distribution system.

FIGURE 7
Number of reduced power flow calculation.

FIGURE 8
Comparison of power loss in each period before and after reconfiguration.

FIGURE 9
Comparison of lowest bus voltage in each period before and after reconfiguration.

TABLE 1 Reconfiguration results in Case 1.

Natural periods	1–8	9–21	22–24
Reconfiguration without coordination	$B_9, B_{14}, B_{28}, B_{33}, B_{36}$	$B_7, B_9, B_{14}, B_{28}, B_{32}$	$B_7, B_9, B_{14}, B_{28}, B_{32}$
Reconfiguration through dynamic coordination	$B_7, B_9, B_{14}, B_{28}, B_{32}$	$B_7, B_9, B_{14}, B_{28}, B_{32}$	$B_7, B_9, B_{14}, B_{28}, B_{32}$

TABLE 2 Comparisons of reconfiguration results in Case 1.

	Before reconfiguration	Static reconfiguration (Ouyang et al., 2009)	Dynamic reconfiguration without coordination (Liu et al., 2020)	Proposed method
Total energy loss (kWh)	1763.15	1,249.60	1,212.20	1,214.39
Number of switching operations	0	4	6	5
Lowest bus voltage (p.u)	0.9147	0.9434	0.9434	0.9434
Operational cost ($)	1,234.21	914.72	908.54	900.07

TABLE 3 Comparison of voltage results.

Natural periods	Bus voltage with BFS			Bus voltage with PFSM		
	Mean value (kV)	Variance (kV)	Lowest value (kV)	Mean value (kV)	Variance (kV)	Lowest value (kV)
1	12.5525	0.0004	12.5512	12.5525	0.0004	12.5512
5	12.5010	0.0002	12.5004	12.5010	0.0002	12.5004
10	12.1524	0.0035	12.1418	12.1524	0.0035	12.1418
15	12.1266	0.0005	12.1250	12.1266	0.0005	12.1250
19	12.0514	0.0008	12.0491	12.0514	0.0005	12.0499
24	12.5018	0.0003	12.5011	12.5018	0.0002	12.5014

$$min\, F_v = \sum_{i=1}^{N_n} \sum_{t'=1}^{N_T} \left(Var\left(P_{E,N_i,t'}\right) + Var\left(Q_{E,N_i,t'}\right) \right),$$

where F_v is the sum of variances of all load power in each interval, N_n is the total number of nodes, N_T is the total number of reconfiguration intervals, and $P_{E,N_i,t'}$ and $Q_{E,N_i,t'}$ are the equivalent active and reactive loads of node i in interval t', respectively.

In addition, reconfiguration interval divisions must satisfy the following constrains:

$$N_T \le N_T^{max},$$

$$S_{t'} - S_{t'-1} \ge \Delta\tau^{min}, t' = 1, 2, \ldots, N_T,$$

$$1 \le S_{t'} \le \tau, t' = 1, 2, \ldots, N_T,$$

where N_T^{max} is the maximum reconfiguration number within a day, $S_{t'-1}$ and $S_{t'}$ are the start natural period and end natural period in interval t', and $\Delta\tau^{min}$ is the minimum natural period in a reconfiguration interval.

Equations 13–16 constitute a typical integer programming model with constraints. The branch and bound algorithm is applied to obtain the best reconfiguration interval division schemes as the number of control variables is limited.

4.2 Static reconfiguration model for single time interval

The network loss $P_{loss,t}$ in natural period t can be described as

$$P_{loss,t} = \sum_{B_k \in L} r_{B_k} \frac{P_{B_k,t}^2 + Q_{B_k,t}^2}{U_{B_k,t}^2},$$

where $P_{B_k,t}$ and $Q_{B_k,t}$ are the active and reactive power at the end terminal of branch B_k in period t, $U_{B_k,t}$ is the end terminal voltage of branch Bk in period t, and L represents the set of all branches.

The objective of static reconfiguration in a single interval is to minimize the total power loss:

$$min\, E_{loss,m} = \sum_{t=s_1^m}^{s_{ns}^m} P_{loss,t} \Delta t,$$

where $E_{loss,m}$ is the total power loss in interval m, Δt is the length of a natural period, s_1^m is the first natural period of the interval m, and ns is the number of natural periods in interval m.

The following constraints should be satisfied during static network reconfiguration:
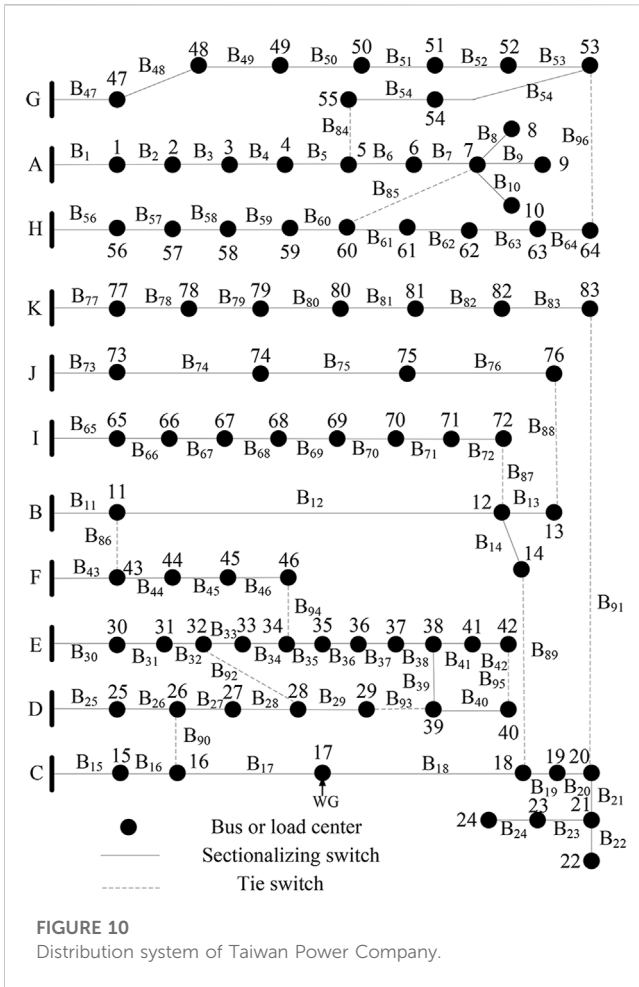
FIGURE 10
Distribution system of Taiwan Power Company.

(1) Radial and connective network constraint.

The distribution network must have radial topology with all of nodes energized.

(2) Permissible range of bus voltage.

When the impact of the power fluctuation of the DGs and loads on the node voltage is considered, the voltage constraint can be described as:

$$\begin{cases} U_{i,t}^{rad,min} \geq U_{min} \\ U_{i,t}^{rad,max} \leq U_{max} \end{cases},$$

where U_{min} and U_{max} are the lower and upper limits of the bus voltage, respectively, and $U_{i,t}^{rad,min}$ and $U_{i,t}^{rad,max}$ are the minimum and maximum voltages of node i in natural period t, considering the power fluctuation of the DGs and loads at a certain confidence level.

(3) Branch power limits.

Taking the uncertainties of DGs and loads into account, the branch power constraint can be described as:
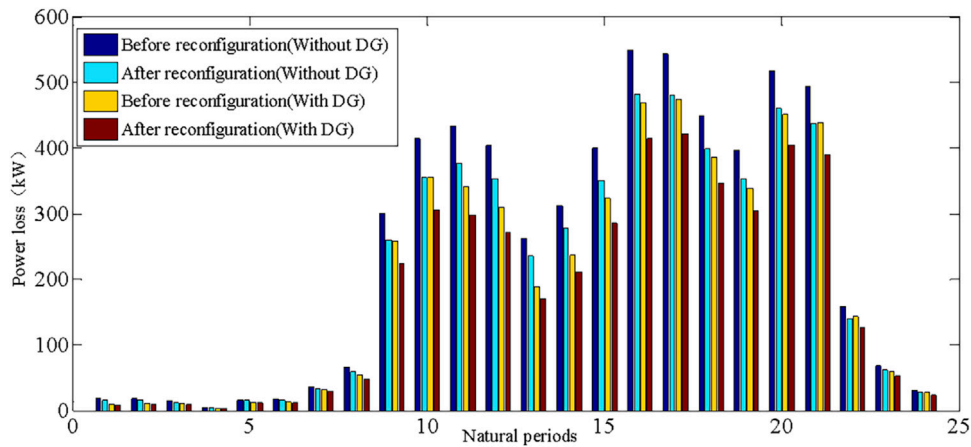
$$S_{B_k,t}^{rad,max} \leq S_{B_k}^{max},$$

where $S_{B_k}^{max}$ is the permitted maximum power transmitted through branch B_k, and $S_{B_k,t}^{rad,max}$ is the maximum power of branch B_k in natural period t, considering the power fluctuation of the DGs and loads at a certain confidence level.

4.3 Improved genetic algorithm

4.3.1 Genetic encoding and decoding

In this study, the randomly arranged branch sequence is regarded as a chromosome by the strategy of searching random spanning trees based on the decimal coding method (Ouyang et al., 2009). In addition, the states of the switches can be obtained by the decoding process. As for the simple network shown in Figure 3, branch B_1 and B_5 do not take part in genetic encoding. The random combination of states of switches at the other branches forms a chromosome, such as R_1: B_2-B_3-B_4-B_8-B_9-B_{12}-B_6-B_7-B_{10}-B_{11}. According to the strategy of searching random spanning trees,

TABLE 4 Reconfiguration results in Case 2.

Natural periods	1–8	9–21	22–24
Reconfiguration without coordination	B_7, B_{13}, B_{34}, B_{42}, B_{55}, B_{62}, B_{72}, B_{83}, B_{86}, B_{89}, B_{90}, B_{92}, B_{93}	B_7, B_{13}, B_{33}, B_{39}, B_{42}, B_{55}, B_{62}, B_{72}, B_{83}, B_{86}, B_{89}, B_{90}, B_{92}	B_7, B_{88}, B_{33}, B_{39}, B_{42}, B_{55}, B_{62}, B_{72}, B_{83}, B_{86}, B_{89}, B_{90}, B_{92}
Reconfiguration through dynamic coordination	B_7, B_{13}, B_{34}, B_{39}, B_{42}, B_{55}, B_{62}, B_{72}, B_{83}, B_{86}, B_{89}, B_{90}, B_{92}	B_7, B_{13}, B_{34}, B_{39}, B_{42}, B_{55}, B_{62}, B_{72}, B_{83}, B_{86}, B_{89}, B_{90}, B_{92}	B_7, B_{13}, B_{34}, B_{39}, B_{42}, B_{55}, B_{62}, B_{72}, B_{83}, B_{86}, B_{89}, B_{90}, B_{92}

TABLE 5 Comparisons of reconfiguration results in Case 2.

	Before reconfiguration	Static reconfiguration (Ouyang et al., 2009)	Dynamic reconfiguration without coordination (Liu et al., 2020)	Proposed method
Total energy loss (kWh)	4,915.25	4,530.63	4,381.79	4,382.13
Number of switching operations	0	9	11	9
Lowest bus voltage (p.u)	0.9313	0.9510	0.9510	0.9510
Operational cost ($)	3,440.68	3,261.44	3,177.25	3,157.49

FIGURE 11
Comparison of power loss in each period before and after reconfiguration.
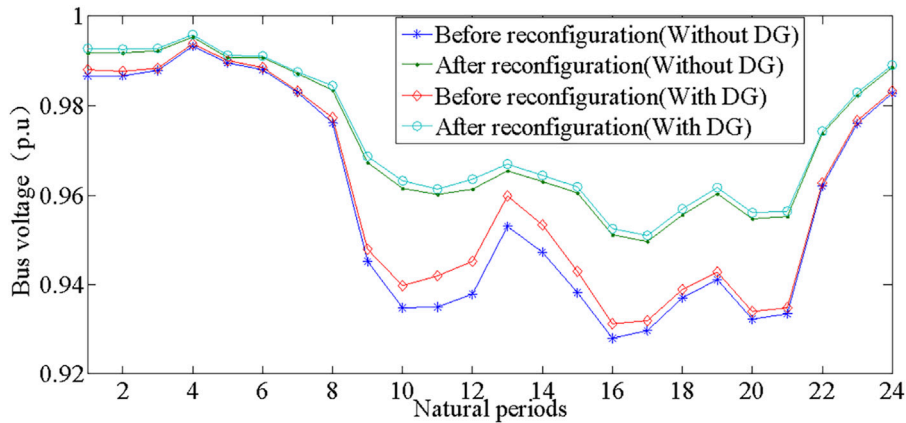
FIGURE 12
Comparison of lowest bus voltage in each period before and after reconfiguration.

the spanning tree corresponding to chromosome R_1 should be: B_1-B_2-B_3-B_4-B_8-B_9-B_{12}-B_6-B_{10}-B_5.

4.3.2 Detection of offspring chromosome

The most time-consuming part in the process of reconfiguration is the fitness calculation of chromosomes, which represents different reconfiguration schemes. There are a certain number of same individuals between the offspring and parent population after cross and mutation operations. The fitness of these individuals in the offspring population can be obtained directly from the parent population, thus avoiding time-consuming power flow calculation. Therefore, a hash table is designed to store the individuals' fitness, and the length of the hash table is the same as the size of the population. To enhance the efficiency of table querying, the set of open switches of individuals is used to represent the individual. For the network in Figure 3, the open switch set of chromosome R1 is {B7, B11}, so B7–B11 is stored in the hash table to represent R1. Figure 4 shows the detection process of the offspring

chromosome. As B7–B11, which represents R1, is included in the parent chromosomes, the fitness of R1 can be obtained from the parent population.

4.3.3 Selection operation

The elitist strategy is applied in the selection operation, and the merging of the offspring and parent population increases the number of good individuals. The tournament algorithm is used in the merged population. Two individuals are chosen successively from all the chromosomes, and the one whose fitness is larger is selected.

4.3.4 Crossover operation

The order-based crossover method is applied in this study. First, two points of one chromosome are chosen to be cut off randomly. Then, the position of the first point is taken as the starting point and the genes between the two points are put into another chromosome. The repeating genes of the new chromosome are removed to get the next generation.

4.3.5 Mutation operation

Two points of one chromosome are chosen randomly and the genes between the two points are rearranged in the reverse order to get the new chromosome.

4.3.6 Obtaining target solution set

The solution set of the first iteration in the static reconfiguration is regarded as the initial target solution set. Then, the solution set of each iteration is compared with the target solution set, and the solution with better fitness, which has not appeared in the target solution set, is added into the target solution set.

4.4 Model of dynamic reconfiguration

The objective of the dynamic reconfiguration is to minimize the daily cost of the distribution network, which can be described as

$$min\, F_c = \sum_{m=1}^{N_T} \sum_{t=s_{m-1}}^{s_m} \left(P_{loss,t} \cdot \Delta t \cdot \rho_{E,t} \right) + N_s \cdot C_B,$$

where $\rho_{E,t}$ is the price of power at the natural period t, N_s is the number of switch operations within a day, and C_B is the cost of each switch operation.

The radial and connective network constraint, node voltage constraint, and line load constraint that should be satisfied during static network reconfiguration are also included in the dynamic network reconfiguration.

4.5 Co-evolution algorithm

The daily reconfiguration schedule constitutes the static reconfiguration schedule at each interval and cannot be guaranteed to be the best since it ignores the interaction between different static reconfiguration schedules. It is necessary to coordinate the reconfiguration schedule at each interval to get the daily reconfiguration schedule that satisfies all the constraints and has minimal operational cost.

The co-evolutionary algorithm is a kind of optimization algorithm which simulates the co-evolutionary phenomenon in nature. In the multi-population co-evolutionary algorithm, the problem is divided into several sections, and each section is represented by a population. The calculation of the fitness of one individual in a population requires the other population's representative solution that is together with the individual to form a complete solution. In this work, the solution set in each interval represents a population in co-evolutionary algorithm, and the co-evolutionary algorithm is applied to coordinate the reconfiguration schedule of each interval to get the daily reconfiguration schedule. Figure 5 is the flow chart of the co-evolutionary algorithm.

In the process of the multi-population co-evolutionary, the representative solution of every interval constitutes the best reconfiguration schedule. In the first iteration, the solution with the least power loss is temporarily regarded as the representative solution. In the subsequent iteration process, the solution with the least daily cost is regarded as the representative solution.

According to the total operational cost of the chromosomes and the representative solution of the interval, the tournament algorithm is used to select the individuals, amount of representative solutions are used to replace some chromosomes to increase the proportion of the representative solution.

In the process of dynamic coordination, if the daily cost of the new dynamic reconfiguration schedule arises, the current co-evolutionary step is regarded as invalid, and the representative solution of the interval is not updated. Abandoning the invalid representative solution can ensure the evolution along the direction of cost reduction.

5 Case studies

5.1 Case 1

The proposed reconfiguration algorithm is applied to the typical IEEE 33-bus system (Baran and Wu, 1989) as shown in Figure 6. The daily load curve is divided into 24 natural periods. The capacity of the overhead transmission line is 10.5 MV A. The WTs are located at nodes 6 and 23. The PVs are located at nodes 24 and 31. The electric price is 0.7\$/kWh, operational cost of the switch is 10\$ each time, and maximum reconfiguration time within a day is three. According to the principle of 3σ, when the confidence level is 99.73%, the fluctuation range of the voltage is within 7%, and the branch power limits must be satisfied. The population size of genetic algorithm (GA) is 40. The cross rate and mutation rate of GA are 0.15 and 0.1, respectively. The proportion of the representative solutions in each population is 10%. The maximum evolution generation is 20.

The numerical simulations are implemented in MATLAB 2022b with Intel® Core™ i5-8350U CPU. Figure 7 shows the saved times of power flow calculation in the static reconfiguration of each interval. The total number of reduced power flow calculations is 749, and the proportion of the number of reduced power flow calculations in the genetic algorithm is 31.21%, which improves the efficiency of the static reconfiguration.

Figure 8 shows the comparison results of power losses in different scenarios. Before the reconfiguration, the total energy loss is 1,763.15 kWh and operational cost is 1,234.21\$. After the reconfiguration, the total energy loss is 1,212.20 kWh and operational cost is 900.07\$. The energy loss has decreased by 31.25%, and the operational cost has decreased by 25.74%. The proposed DNDR algorithm reduces the energy loss and operational cost effectively. When compared with power losses with and without DGs, it can be concluded that both the DGs and network reconfiguration play important roles in reducing power loss.

Figure 9 shows the comparison results of the lowest bus voltages in different scenarios. Before the reconfiguration, the lowest bus voltage is 0.9147 p.u. After the reconfiguration, the lowest bus voltage is 0.9434 p.u. The proposed dynamic reconfiguration algorithm avoids voltage violations.

Table 1 shows the reconfiguration results with and without interval coordination. Table 2 compares the reconfiguration results of different reconfiguration methods. In the reconfiguration results without interval coordination, the energy loss is 1,212.20 kWh and operational cost is 908.54\$. In the reconfiguration results with interval coordination, the energy loss is 1,214.39 kWh and

operational cost is 900.07$. As the proposed dynamic coordination algorithm considers the operational cost of switches, the daily operational cost is less than that of the reconfiguration results without interval coordination.

Table 3 shows the influence of nodal power fluctuations on the lowest bus voltages. The traditional backward/forward sweep (BFS) algorithm is used to compare the power flow based on the sensitivity model (PFSM). The voltage error between the BFS and PFSM is no more than 0.33%. The branch power error between the BFS and PFSM is no more than 2.6%. It takes 60s to calculate power flow 100 times by BFS, and only 0.75s to calculate power flow 100 times by PFSM. The comparisons of the calculation accuracy and computation time prove the validity of the PFSM.

5.2 Case 2

The distribution system of the Taiwan Power Company (Wang et al., 2018) shown in Figure 10 is tested. The system consists of 11 feeders, 83 normally closed switches, and 13 normally open switches; the rated voltage is 11.4 kV and total active and reactive power loads are 28,350 kW and 20,700 kVar, respectively. The system is assumed to be three-phase balance in this work. The wind generations are installed at nodes 6, 13, 17, 19, 31, 34, 52, 58, 71, 79, and 33. The photovoltaic power generations are installed at nodes 7, 9, 12, 14, 21, 28, 45, 54, 64, and 75. The simulation parameters are the same as that of Case 1, except for the population size of the genetic algorithm that is 80.

Table 4 shows the reconfiguration results with and without interval coordination in Case 2. Table 5 analyzes the reconfiguration results of different reconfiguration methods. Through the proposed reconfiguration algorithm, the total energy loss decreases from 4,915.25 kWh to 4,382.13 kWh and operational cost decreases from 3,440.68$ to 3,157.49$. The lowest bus voltage increases from 0.9313 p.u. to 0.9510 p.u. The proposed DNDR algorithm improves the performance of the distribution networks. In the reconfiguration results without interval coordination, the number of switching operations is 11 and operational cost is 3,177.25$. In the proposed reconfiguration algorithm with interval coordination, the number of switching operations is nine and operational cost is 3,157.49$. The dynamic coordination among the different intervals can reduce the number of switching operations to cut the operational cost.

Figures 11, 12 show the comparative results of power loss and node voltage before and after the dynamic reconfiguration. The simulation results show that the proposed dynamic reconfiguration method can effectively reduce the power loss and improve the voltage levels when the loads are heavy. Moreover, the influences of the DGs on power loss and node voltage are also considered. Before reconfiguration, the lowest node voltages are increased from 0.9291 p.u. to 0.9313 p.u. After reconfiguration, the lowest node voltages are increased from 0.9497 p.u. to 0.9510 p.u. The simulation results show that the appropriate DGs can decrease the net loads, reduce the power losses, and maintain the level of bus voltages.

6 Conclusion

This article presents a dynamic reconfiguration method of the distribution network considering the stochastic variations of loads and DG in power, and the following conclusions are drawn:

1) Both the power loss cost and switch operational cost are considered in the proposed dynamic reconfiguration method. The applied co-evolutionary algorithm can effectively coordinate the reconfiguration schedules among different time intervals to reduce the switch operational cost.
2) The effect of power fluctuation on the operation constraints is considered to ensure operational security. The voltage sensitivity models are used for PFCs, which can improve the computation efficiency of the DNDR.

Data availability statement

The original contributions presented in the study are included in the article/Supplementary Material; further inquiries can be directed to the corresponding author.

Author contributions

QL: conceptualization, formal analysis, methodology, and writing–original draft. LZ: formal analysis, visualization, and writing–review and editing. XJ: methodology and writing–review and editing. HS: supervision and writing–review and editing.

Conflict of interest

The authors declare that the research was conducted in the absence of any commercial or financial relationships that could be construed as a potential conflict of interest.

Publisher's note

All claims expressed in this article are solely those of the authors and do not necessarily represent those of their affiliated organizations, or those of the publisher, editors, and reviewers. Any product that may be evaluated in this article, or claim that may be made by its manufacturer, is not guaranteed or endorsed by the publisher.

References

Gao, H., Ma, W., He, S., Wang, L., and Liu, J. (2022a). Time-segmented multi-level reconfiguration in distribution network: A novel cloud-edge collaboration framework. *IEEE Trans. Smart Grid* 13 (4), 3319–3322. doi:10.1109/TSG.2022.3156433

Gao, H., Ma, W., Xiang, Y., Tang, Z., Xu, X., Pan, H., et al. (2022b). Multi-objective dynamic reconfiguration for urban distribution network considering multi-level switching modes. *J. Mod. Power Syst. Clean. Energy* 10 (5), 1241–1255. doi:10.35833/MPCE.2020.000870

Haghighat, H., and Zeng, B. (2016). Distribution system reconfiguration under uncertain load and renewable generation. *IEEE Trans. Power Syst.* 31 (4), 2666–2675. doi:10.1109/TPWRS.2015.2481508

Harsh, P., and Das, D. (2023). A simple and fast heuristic approach for the reconfiguration of radial distribution networks. *IEEE Trans. Power Syst.* 38 (3), 2939–2942. doi:10.1109/TPWRS.2023.3256136

Hizarci, H., Demirel, O., and Turkay, B. E. (2022). Distribution network reconfiguration using time-varying acceleration coefficient assisted binary particle swarm optimization. *Eng. Sci. Technol. Int. J.* 35, 101230. doi:10.1016/j.jestch.2022.101230

Jakus, D., Čađenović, R., Vasilj, J., and Sarajčev, P. (2020). Optimal reconfiguration of distribution networks using hybrid heuristic-genetic algorithm. *Energies* 13 (7), 1544. doi:10.3390/en13071544

Kianmehr, E., Nikkhah, S., Vahidinasab, V., Giaouris, D., and Taylor, P. C. (2019). A resilience-based architecture for joint distributed energy resources allocation and hourly network reconfiguration. *IEEE Trans. Ind. Inf.* 15 (10), 5444–5455. doi:10.1109/TII.2019.2901538

Liu, Q., Ji, X., and Wang, H. (2020). Dynamic Reconfiguration of active distribution system based on matrix shifting operation and interval merger. *J. Electr. Eng. Technol.* 15, 621–633. doi:10.1007/s42835-020-00356-2

López, J. C., Lavorato, M. J., Franco, F., and Rider, M. J. (2016). Robust optimisation applied to the reconfiguration of distribution systems with reliability constraints. *IET Gener. Transm. Distrib.* 10 (4), 917–927. doi:10.1049/iet-gtd.2015.0558

Lotfi, H., Ghazi, R., and Naghibi-Sistani, M. (2020). Multi-objective dynamic distribution feeder reconfiguration along with capacitor allocation using a new hybrid evolutionary algorithm. *Energy Syst.* 11, 779–809. doi:10.1007/s12667-019-00333-3

Lotfi, H., and Ghazi, R. (2021). Optimal participation of demand response aggregators in reconfigurable distribution system considering photovoltaic and storage units. *J. Ambient. Intell. Hum. Comput.* 12, 2233–2255. doi:10.1007/s12652-020-02322-2

Ouyang, W., Cheng, H., Zhang, X., Yao, L., and Bazargan, M.(March 2009) "Random spanning tree based improved GA for distribution reconfiguration," in Proceedings of the 2009 asia-pacific power and energy engineering conference, Wuhan, China, pp. 1–4. doi:10.1109/APPEEC.2009.4918634

Raj, V., and Kumar, B. K. (2020). A new affine arithmetic-based optimal network reconfiguration to minimize losses in a distribution system considering uncertainty using binary particle swarm optimization. *Electr. Power Compon. Syst.* 48 (6-7), 628–639. doi:10.1080/15325008.2020.1797940

Razavi, S. -M., Momeni, H. -R., Haghifam, M. -R., and Bolouki, S. (2022). Multi-objective optimization of distribution networks via daily reconfiguration. *IEEE Trans. Power Deliv.* 37 (2), 775–785. doi:10.1109/TPWRD.2021.3070796

Roosta, A., Eskandari, H. R., and Khooban, M. H. (2019). Optimization of radial unbalanced distribution networks in the presence of distribution generation units by network reconfiguration using harmony search algorithm. *Neural. comput. Appl.* 31, 7095–7109. doi:10.1007/s00521-018-3507-0

Santos, S. F., Gough, M., Fitiwi, D. Z., Pogeira, J., Shafie-khah, M., and Catalão, J. P. S. (2022). Dynamic distribution system reconfiguration considering distributed renewable energy sources and energy storage systems. *IEEE Syst. J.* 16 (3), 3723–3733. doi:10.1109/JSYST.2021.3135716

Sekhavatmanesh, H., and Cherkaoui, R. (2020). A multi-step reconfiguration model for active distribution network restoration integrating dg start-up sequences. *IEEE Trans. Sustain Energy* 11 (4), 2879–2888. doi:10.1109/TSTE.2020.2980890

Song, Y., Zheng, Y., Liu, T., Lei, S., and Hill, D. J. (2020). A new formulation of distribution network reconfiguration for reducing the voltage volatility induced by distributed generation. *IEEE Trans. Power Syst.* 35 (1), 496–507. doi:10.1109/TPWRS.2019.2926317

Sun, S., Li, G., Chen, C., Bian, Y., and Bie, Z. (2023). A novel formulation of radiality constraints for resilient reconfiguration of distribution systems. *IEEE Trans. Smart Grid* 14 (2), 1337–1340. doi:10.1109/TSG.2022.3220054

Wang, S., Liu, Q., and Ji, X. (2018). A fast sensitivity method for determining line loss and node voltages in active distribution network. *IEEE Trans. Power Syst.* 33 (1), 1148–1150. doi:10.1109/TPWRS.2017.2735898

Zhan, J., Liu, W., Chung, C. Y., and Yang, J. (2020). Switch opening and exchange method for stochastic distribution network reconfiguration. *IEEE Trans. Smart Grid* 11 (4), 2995–3007. doi:10.1109/TSG.2020.2974922

Zhang, C., Liu, Q., Zhou, Bin., Chung, C. Y., Li, J., Zhu, L., et al. (2023). A central limit theorem-based method for DC and AC power flow analysis under interval uncertainty of renewable power generation. *IEEE Trans. Sustain. Energy* 14 (1), 563–575. doi:10.1109/TSTE.2022.3220567

Zheng, W., Huang, W., Hill, D. J., and Hou, Y. (2021a). An adaptive distributionally robust model for three-phase distribution network reconfiguration. *IEEE Trans. Smart Grid* 12 (2), 1224–1237. doi:10.1109/TSG.2020.3030299

Zheng, W., Huang, W., Hill, D. J., and Hou, Y. (2021b). An adaptive distributionally robust model for three-phase distribution network reconfiguration. *IEEE Trans. Smart Grid* 12 (2), 1224–1237. doi:10.1109/TSG.2020.3030299